Field induced crossover in antiferromagnetic spin-frustrated clusters: Influence of static and dynamic structural deformations

Alex Tarantul [a], Boris Tsukerblat [a,*], Achim Müller [b]

[a] *Department of Chemistry, Ben-Gurion University of the Negev, P.O. Box 653, 84105 Beer-Sheva, Israel*
[b] *Fakultät für Chemie, Universität Bielefeld, 33501 Bielefeld, Germany*

ABSTRACT

We propose a theoretical study of the magnetic behavior of spin frustrated trinuclear clusters in the region of the field induced crossover of the levels which are crucial for the description of the static magnetization and dynamic behavior in a sweeping field. The emphasis is made on a competitive role of the antisymmetric (AS) exchange and static structural distortions of the metal center network as well as on the consequences of the dynamic pseudo Jahn–Teller (JT) instability that is closely related to spin frustration. The structural conformations are shown to be controlled by the magnetic field in the anticrossing region (magnetoelastic coupling). We employ the three-spin model for the cluster anion present in $K_6[V_{15}^{IV}As_6O_{42}(H_2O)] \cdot 8H_2O$ (V_{15} cluster) and analyze the role of different components of AS exchange in the shape of the magnetic susceptibility vs field. Both types of deformations (static and dynamic) are shown to be competitive to the AS exchange and tend to reduce the magnetic anisotropy caused by the AS exchange.

© 2008 Elsevier B.V. All rights reserved.

1. Introduction

The discovery of single molecular magnetism in large magnetic clusters, objects of "zero-dimensional" magnetism, [1–8] has given a strong impact to the related studies of spin levels, especially with regard to magnetic anisotropies [9–15] and relaxation processes [16,17]. High-spin molecules like the classical single molecule magnet Mn_{12}–acetate ($Mn_{12}O_{12}$ $(OAc)_{16}(H_2O)_4$) [1,7] possess a high-spin ($S = 10$) ground state and negative magnetic anisotropy that result in a significant barrier for spin reorientation. This gave rise to the new field of molecular magnetism that is promising for the important applications, like memory storage unit of molecular size in context with quantum computation (see Ref. [1] and review article [7] highlighting this field).

During the past decade much attention has been attracted by a comparable large cluster anion present in $K_6[V_{15}^{IV}As_6O_{42}(H_2O)] \cdot 8H_2O$ (hereafter V_{15}) containing 15 ions V^{IV} ($S_i = 1/2$) that are strongly coupled through antiferromagnetic exchange interaction via oxo-bridges (D_{3d} structure of the whole molecule). The V_{15} cluster was discovered almost 20 years ago [18] and since that time attracts continuous and increasing attention (ca. 60 publications) as an unique molecular magnet exhibiting three magnetic layers, central spin triangle and two almost spin paired spin hexa-

gons. Studies of the adiabatic magnetization and quantum dynamics of V_{15} cluster [19–24] showed that this system exhibits a hysteresis loop of magnetization of molecular origin and can be referred to as a mesoscopic system. Recently the low spin V_{15} molecular magnet has been mentioned as a promising candidate to create long living memory units for quantum computing [25,26]. Realization of potential applications of the nanomagnetic materials, in particular, qubit implementation, requires a detailed theoretical and experimental investigation of the wave functions and energy patterns of large magnetic clusters.

Low lying spin excitations of the V_{15} system affecting the low temperature magnetic ($T < 100$ K) properties [19] and inelastic neutron scattering [27,28] can be treated within the model of a spin-frustrated triangular unit [29–31] formed by a central magnetic layer only weakly coupled to spin hexagons (Fig. 1). Spin frustration is inherently related to orbital degeneracy of the system and the ground state of the V_{15} cluster is represented by the orbital doublet ^2E [32]. In this context, there is a need for a deeper understanding of the crucial role of AS exchange (Dzyaloshinsky–Moriya interaction [33,34]) in spin-frustrated systems [32] – especially in the V_{15} cluster [36–39] and of the importance of even weak concurring perturbations like structural distortions [40] and dynamical distortions caused by spin–vibronic JT interactions. The latter gives rise to a structural instability [39] with spontaneous symmetry lowering. The deviation from the trigonal type symmetry in V_{15} molecule has been indicated in [27,28] on the basis of inelastic

* Corresponding author. Tel.: +972 8 647 93 61; fax: +972 8 647 29 43.
E-mail address: tsuker@bgu.ac.il (B. Tsukerblat).
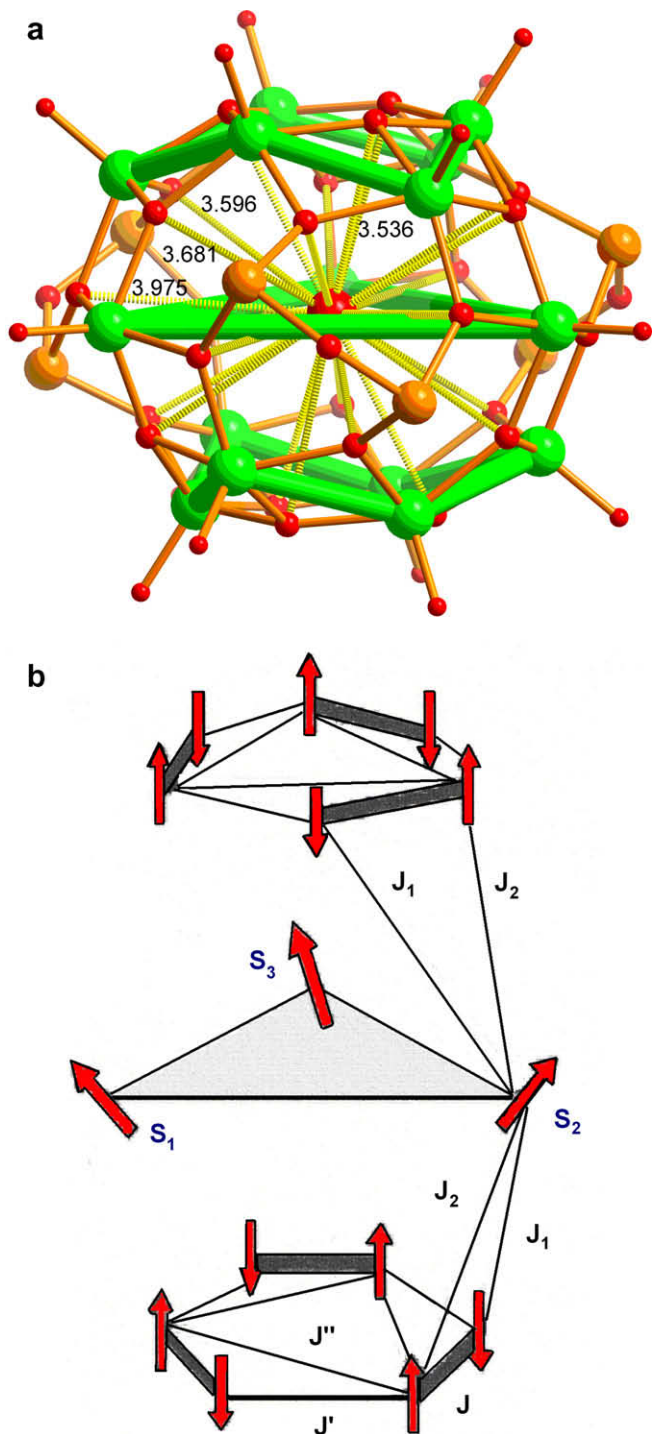
Fig. 1. (a) Structure of the cluster anion of $K_6[V_{15}^{IV}As_6O_{42}(H_2O)]^{6-}$ with D_{3d} symmetry in ball-and-stick representation: V, green; As, orange; O, red, central red ball, water molecule. The metal network is highlighted by thick green lines. The magnetic layers are formed by the V_3 triangle sandwiched by two distorted V_6 hexagons (interatomic distances in Å). (b) scheme of spin arrangements in the ground state when the spins of the external hexagons are paired and the spins of the central triangle are frustrated. (For interpretation of the references to colour in this figure legend, the reader is referred to the web version of this article.)

neutron scattering data and attributed to the influence of the water molecule located in the center of the spherical cavity of V_{15} or to the presence of the water in the structure of the crystal lattice. The coexistence of AS exchange and small distortions (so-called J-strain) was recently found [41–46] to be relevant for many trian-

gular spin-frustrated systems (detailed study of a series of triangular vanadium clusters is given in Ref. [42]).

In this article, we report on the interplay between the AS exchange, scalene structural and JT distortions in the trinuclear spin-frustrated clusters with the emphasis on the crossing/anticrossing region of the magnetic sublevels. This region is important for the description of the half-step magnetization in triangular spin-frustrated clusters [19,38,41–47], dynamical behavior of magnetization [20] in a sweeping field and magnetoelastic instability resulting in the field induced cooperative phenomena in the molecule based magnets [48]. We show that AS exchange on the one hand and both kinds of mentioned distortions on the other hand show competitive influence on the magnetic anisotropy of spin-frustrated trinuclear clusters. We also demonstrate that the JT conformations can be efficiently controlled by variation of the magnetic field in the crossover area. In the series of sample calculations the available parameters for the V_{15} system are used.

2. The Hamiltonian: spin levels in a static model

The full Hamiltonian of the slightly distorted trinuclear system, Eq. (1), includes isotropic exchange interaction in a symmetric trigonal system (first term, H_0), a selected static Scalene structural distortion (J-strain along side 12) represented by the second term (H_d), AS exchange (H_{AS}), (third term) Hamiltonian of the free harmonic vibrations (H_v) of the metal core, spin–vibronic coupling (term H_{sv}) and isotropic Zeeman interaction (last term, H_{Zeem}):

$$H = 2J \sum_{i,k=1,2,3} \mathbf{S}_i \mathbf{S}_k + 2\delta \mathbf{S}_1 \mathbf{S}_2 + \sum_{i,k} \mathbf{D}_{ij}[\mathbf{S}_i \times \mathbf{S}_k] + H_v + H_{sv} + g\beta\mathbf{H}\sum_i \mathbf{S}_i.$$
(1)

In this Section, we will focus on the results of the static model and consider thus only spin–spin interactions while the vibronic effects will be considered separately in Section 3. In the definition of the isotropic exchange in Eq. (1), the parameter J is positive for the antiferromagnetic V_{15} system. Since the main contribution to the magnetic anisotropy is provided by the AS exchange, for the sake of simplicity the g-factor is assumed to be isotropic. Also, since the deviation from the trigonal symmetry is supposed to be relatively small ($|\delta| \ll J$), both H_d and H_{AS} contributions will be considered to be first order perturbations. In this sense, the influence of deformation on AS exchange may be neglected as a second order effect and we will employ the following expression for H_{AS} that is invariant under the symmetry operations in D_{3d} point group:

$$
\begin{aligned}
H_{AS} = &\, D_n([\mathbf{S}_1 \times \mathbf{S}_2]_Z + [\mathbf{S}_2 \times \mathbf{S}_3]_Z + [\mathbf{S}_3 \times \mathbf{S}_1]_Z) \\
&+ D_l\left([\mathbf{S}_1 \times \mathbf{S}_2]_X - \frac{1}{2}[\mathbf{S}_2 \times \mathbf{S}_3]_X + \frac{\sqrt{3}}{2}[\mathbf{S}_2 \times \mathbf{S}_3]_Y \right. \\
&\left. -\frac{1}{2}[\mathbf{S}_3 \times \mathbf{S}_1]_X - \frac{\sqrt{3}2}{[}\mathbf{S}_3 \times \mathbf{S}_1]_Y \right) \\
&+ D_t\left([\mathbf{S}_1 \times \mathbf{S}_2]_Y - \frac{\sqrt{3}}{2}[\mathbf{S}_2 \times \mathbf{S}_3]_X - \frac{1}{2}[\mathbf{S}_2 \times \mathbf{S}_3]_Y \right. \\
&\left. +\frac{\sqrt{3}}{2}[\mathbf{S}_3 \times \mathbf{S}_1]_X - \frac{1}{2}[\mathbf{S}_3 \times \mathbf{S}_1]_Y \right)
\end{aligned}
$$
(2)

where the components of the vector operators refer to the molecular frame as shown in Fig. 2. One can see that the vector parameters $\mathbf{D}_{ik}(ik = 12, 21, 31)$ in a trigonal system can be expressed in terms of three effective components of the AS exchange vector [35], namely along and perpendicular to sides (in plane of the triangle) and perpendicular to the plane components whose absolute values are D_l, D_t and D_n, respectively (Fig. 2). It is important to note that in trigonal systems only two effective parameters, namely, the normal part D_n and the combined in-plane parameter $D_\perp = \sqrt{D_l^2 + D_t^2}$, have
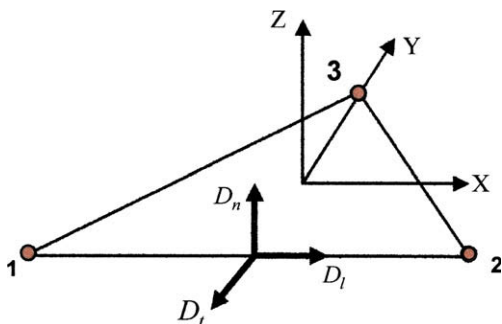
Fig. 2. Molecular frame and definition of the AS exchange parameters in a triangular V_3 unit.

physical significance; this means that in a strictly trigonal system (belonging to any point group involving C_3 axis) the parameters D_l and D_t are undistinguishable in magnetic and spectroscopic measurements.

The energy pattern produced by the isotropic part of the exchange interaction ($H_0 + H_d$) for $S_i = 1/2$ triangular system consists of two spin-doublets separated by the gap $2|\delta|$ and a spin-quadruplet:

$$E(S_{12}, S) = J[S(S+1) - 9/4] + \delta[S_{12}(S_{12}+1) - 3/2], \quad (3)$$

where S is the full spin of the system ($S = 1/2, 3/2$), S_{12} is the intermediate spin in the three-spin coupling scheme ($S_{12} = 0, 1$) and the zero-field gap $E(1, 1/2) - E(0, 1/2) = 2\delta$. Fig. 3 (in the plots we use the isotropic exchange parameter $J = 0.85$ cm^{-1} found for V$_{15}$ [19]) shows the Zeeman levels pattern for the in-plane direction of the field when the anisotropic effect of the AS exchange is most pronounced and the experimental data on magnetization are available [19,43]. In the case of a symmetric system ($\delta = 0$) one finds two eigen-values of H_0 corresponding to full spin values $S = 1/2$ ("accidentally" degenerate ground state [32] in the case of antiferromagnetic coupling) and $S = 3/2$ that are crossed at the field $H_{cr} = 3J/g\beta$ (Fig. 3a). When the distortion is involved the two crossing points occur at the fields $H_{c1} = 3J/g\beta$ and $H_{c2} = (3J + 2\delta)/g\beta$ as shown in Fig. 3b (the crossover area under consideration is marked in Fig. 3b and c). Since only the isotropic part of the Hamiltonian is employed the splittings in Fig. 3a and b are independent of the field direction. Finally, Fig. 3c shows the energy pattern when both distortion and AS exchange are operative. In this case, the ground state splitting appears as a combined effect of both distortion and AS exchange

and can be approximately (up to second order corrections) presented as $\Delta' = \sqrt{4\delta^2 + 3D_n^2 - (D_t^2 + D_l^2)/8J}$. The main (first order) contribution to the zero-field gap is provided by the normal component of the AS exchange and distortion while the in-plane component gives a second order contribution caused by the mixing of spin-doublet and spin-quadruplet levels. The pattern of the magnetic sublevels in the crossover region strongly depends on the interrelation between the distortion parameter and components of the AS exchange.

It is worthwhile to consider the Zeeman energy pattern in the crossover $S = 1/2$, $M_S = -1/2$ and $S = 3/2$, $M_S = -3/2$ region within the perturbation theory keeping in mind that $|D_n|$, $|D_l|$, $|D_t|$, $|\delta| \ll J$. To construct the full Hamiltonian matrix, we will use the restricted basis set composed of three eigen-functions of the unperturbed Hamiltonian H_0 corresponding to the three crossing levels. When a strong field ($g\beta H \gg |D_n|$) is oriented in the plane the AS exchange is fully reduced [37] and one can alternatively use the wave functions $|(S_{12})SM_\perp\rangle$ corresponding to the intersection region that means that the quantization axis is located in the plane (this is indicated by the symbol $\perp$):

$$\left|(1)\frac{1}{2}, M_\perp = -\frac{1}{2}\right\rangle = -\frac{\sqrt{2}}{2}\left(\left|(1)\frac{1}{2}, \frac{1}{2}\right\rangle - \left|(1)\frac{1}{2}, -\frac{1}{2}\right\rangle\right)$$

$$\left|(0)\frac{1}{2}, M_\perp = -\frac{1}{2}\right\rangle = -\frac{\sqrt{2}}{2}\left(\left|(0)\frac{1}{2}, \frac{1}{2}\right\rangle - \left|(0)\frac{1}{2}, -\frac{1}{2}\right\rangle\right)$$

$$\left|(1)\frac{3}{2}, M_\perp = -\frac{3}{2}\right\rangle = \frac{\sqrt{2}}{4}\left(\left|(1)\frac{3}{2}, \frac{3}{2}\right\rangle - \left|(1)\frac{3}{2}, -\frac{3}{2}\right\rangle\right) \quad (4)$$

$$- \frac{\sqrt{6}}{4}\left(\left|(1)\frac{3}{2}, \frac{1}{2}\right\rangle - \left|(1)\frac{3}{2}, -\frac{1}{2}\right\rangle\right).$$

Using the irreducible tensor operators technique one can find the following matrix representation of the full Hamiltonian in the restricted basis set, Eq. (4):

$$\begin{pmatrix} (-3J - g\beta H)/2 + \delta & 0 & -3D_l/4\sqrt{2} \\ 0 & (-3J - g\beta H)/2 - \delta & -3D_t/4\sqrt{2} \\ -3D_l/4\sqrt{2} & -3D_t/4\sqrt{2} & (-3J - 3g\beta H)/2 + \delta \end{pmatrix}. \quad (5)$$

One can see that the normal component of AS exchange does not affect the behavior of the magnetic sublevels in the crossing region in the first order approximation (as it was found for the symmetric systems [38]). The normal part of the AS exchange was shown [35,38] to contribute (along with the distortion) to the zero-field
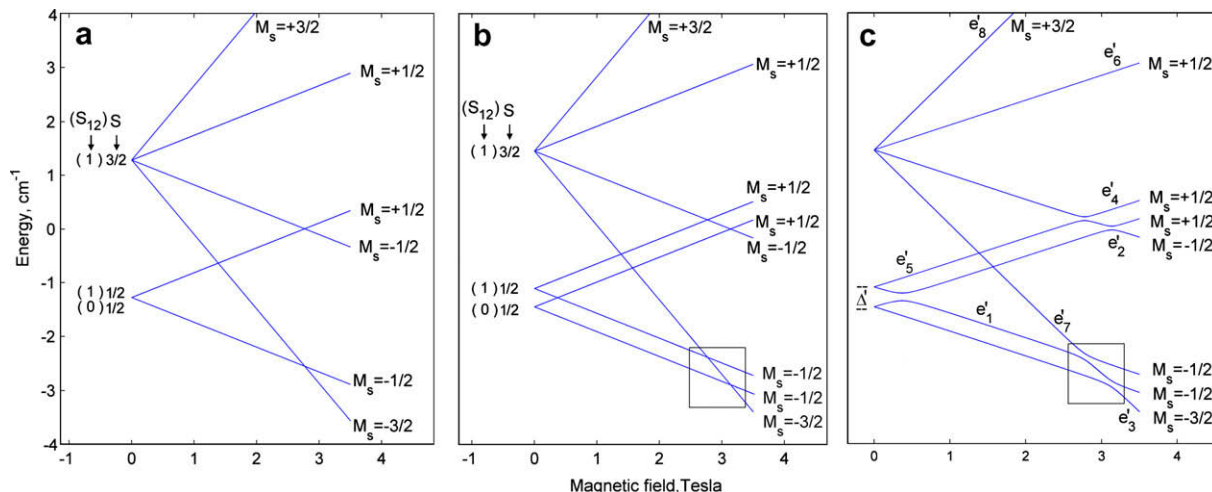

Fig. 3. Energy levels of a $S_i = 1/2$ triangular unit in the perpendicular ($\boldsymbol{H} \perp C_3$) field, M_S labels are related to quantization axis along the field: (a) $J = 0.85$ cm^{-1}, $\delta = 0$, $D_n = D_\perp = 0$; (b) $J = 0.85$ cm^{-1}, $\delta = +0.2J$, $D_n = D_\perp = 0$; (c) $J = 0.85$ cm^{-1}, $\delta = +0.2J$, $D_n = 0.1J$, $D_t = 0.08J$, $D_l = 0.13J$, M_S labels correspond to a strong field limit.

splitting and magnetic anisotropy at low-fields. On the contrary, the energy pattern in the crossover region is affected (up to high order corrections) by the in-plane components of the AS exchange. The eigen-values of the matrix, Eq. (5), have simple analytical forms when only one of two in-plane components of AS exchange is non-zero. In these particular cases, the energy levels in the anticrossing region (within the designated area in Fig. 3c) are the following (we give here the results for $\delta > 0$):

Case 1: $D_l \neq 0$, $D_t = 0$:

$$v_1(H) = -3J/2 - \delta - \beta g H/2$$

$$v_{2,3}(H) = -\beta g H \mp \sqrt{9D_l^2/32 + (3J/2 - \beta g H/2)^2} + \delta. \tag{6}$$

Case 2: $D_t \neq 0$, $D_l = 0$:

$$u_1(H) = -3J/2 + \delta - \beta g H/2$$

$$u_{2,3}(H) = -\beta g H \mp \sqrt{9D_t^2/32 + (3J/2 - \beta g H/2 + \delta)^2}. \tag{7}$$

One can join these solutions and get approximate analytical expressions for the energy levels in a more common case, i.e. when both D_t and D_l are non-zero:

$$e_3'(H) \approx -g\beta H - \sqrt{9D_t^2/32 + (3J/2 - \beta g H/2 + \delta)^2},$$

$$e_7'(H) \approx -g\beta H + \sqrt{9D_t^2/32 + (3J/2 - \beta g H/2)^2} + \delta,$$

$$e_1'(H) \approx -3J/2 - g\beta H/2 + \sqrt{9D_t^2/32 + (3J/2 - \beta g H/2 + \delta)^2}$$
$$- \sqrt{9D_l^2/32 + (3J/2 - \beta g H/2)^2}. \tag{8}$$

The results for $\delta < 0$ can be obtained from Eq. (8) by the substitution $\delta \to -\delta$, $D_t \to D_l$, $D_l \to D_t$. Eq. (8) provides a very good accuracy for the levels in the anticrossing area until $|D_t|$, $|D_l|$ become too small ($\approx 0.01J$) and these formulas lose their accuracy.

Fig. 3c shows that AS exchange in conjunction with distortion of the triangle produce avoided crossing with a peculiar non-linear behavior at low-field **H** in the plane of the triangle. The details of anticrossing which affect static and dynamic magnetic behavior of the system are essentially dependent on the interrelation between the components of the AS exchange as shown in Fig. 4. The results can be summarized as follows: (1) in-plane components of the AS exchange D_t and D_l result in the avoided crossing so that the behavior of the levels is determined by the interrelation between D_t, D_l, δ and signs of these parameters; (2) if one of two components of the in-plane AS exchange in the distorted system ($\delta \neq 0$) is non-zero (either D_t or D_l) the energy pattern exhibits one crossing point and one avoided cross-
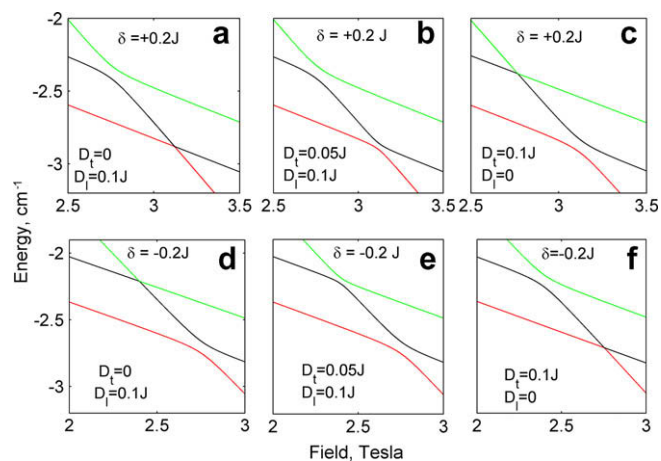

Fig. 4. Influence of the D_t, D_l components on the behavior of spin levels in the anticrossing region, $J = 0.85$ cm^{-1}, $\delta = +0.2J$, $D_n = 0.1J$; M_S labels are indicated in Fig. 3.

ing. The shape of the magnetization step essentially depends on the character of the intersection of the low lying levels. One can see that providing $\delta > 0$ and $D_t = 0$, $D_n \neq 0$ the exact crossing occurs in the ground state (Fig. 4a) while if $D_t \neq 0$, $D_n = 0$ one can observe an avoided crossing (Fig. 4c). Providing $\delta < 0$ the anticrossing point occurs in the ground state if $D_t \neq 0$, $D_n = 0$; (3) when all involved perturbations are non-zero the energy pattern exhibits two avoided crossing points with different minimal gaps (Fig. 4b and e); (4) the energy pattern possesses a remarkable symmetry property: this pattern is invariant under simultaneous replacement $\delta \to -\delta$, $D_t \to D_l$, $D_l \to D_t$ (compare pairs Fig. 4a, f and c, d). This implies a principal restriction to a possibility of experimental determination of the named parameters from the experimental data. Finally, it should be underlined that due to symmetry lowering the in-plane parameters D_t and D_l act independently meanwhile in a symmetric system they are indistinguishable and concur as an only combined parameter $D_\perp = \sqrt{D_n^2 + D_t^2}$. One can see that combined action of the distortion and AS exchange results in a new anticrossing pattern, in particular, in new rules for the crossing, that are essentially different from those in a symmetric model (see Ref. [35]).

3. Field induced Jahn–Teller instability in the crossing region

The problem of JT structural instability in the orbitally degenerate ground spin-frustrated state has been considered in [39]. Since the anticrossing area is represented by a set of quasi-degenerate levels the pseudo JT interaction induced by a strong applied magnetic field can be active and acts along with the AS exchange and static structural distortions. In this case in correspondence with the general statements of the theory [49–51] under some conditions JT coupling can give rise to a structural instability and spontaneous lowering of symmetry. For this reason, in this Section we will consider such a kind of dynamical distortions that are associated with the vibronic pseudo JT coupling.

The exchange parameters are functions of the metal–metal distances so the linear terms of the vibronic Hamiltonian can be represented as:

$$H_{sv} = 2 \sum_{ij} \mathbf{S}_i \mathbf{S}_j \sum_{\alpha=1,x,y} \left(\frac{\partial J_{ij}(R_{ij})}{\partial R_{ij}} \right)_{\Delta R_{ij}=0} \cdot \frac{\partial R_{ij}}{\partial Q_\alpha} Q_\alpha, \tag{9}$$

where $\partial J_{ij}(R_{ij})/\partial R_{ij}$ are derivatives of the isotropic exchange and ΔR_{ij} are changes of the metal–metal distances in the course of vibrations and the summation is extended over all pairwise spin–spin interactions. The main contribution to the vibronic interaction arises from the modulation of the leading isotropic exchange by the JT displacements of the E-type (double degenerate mode Q_X, Q_Y, see their explicit forms, for example, in [52]) of spin sites and by the full-symmetric vibration (normal coordinate Q_A), while the anisotropic contributions are small [39]. The corresponding spin-vibronic Hamiltonian can be presented as:

$$H_{sv} = \lambda(\hat{V}_A Q_A + \hat{V}_x Q_x + \hat{V}_y Q_y), \tag{10}$$

where $\lambda = (\partial J_{ij}(R_{ij})/\partial R_{ij})_{\Delta R_{ij}=0}$ and the symmetry adapted operators of spin–vibronic coupling $\hat{V}_i$ for the involved types of vibrations are found as:

$$\hat{V}_A = \sqrt{\frac{2}{3}}(\mathbf{S}_2\mathbf{S}_3 + \mathbf{S}_3\mathbf{S}_1 + \mathbf{S}_1\mathbf{S}),$$

$$\hat{V}_x = \frac{1}{\sqrt{6}}(\mathbf{S}_2\mathbf{S}_3 + \mathbf{S}_3\mathbf{S}_1 - 2\mathbf{S}_1\mathbf{S}), \tag{11}$$

$$\hat{V}_y = \frac{1}{\sqrt{2}}(\mathbf{S}_2\mathbf{S}_3 - \mathbf{S}_3\mathbf{S}_1).$$

These expressions show that within the approximation so far adopted the spin–vibronic interaction involves only scalar products of spin operators and therefore proves to be magnetically isotropic. The 3×3-matrix of the full Hamiltonian, i.e. adiabatic Hamiltonian $\mathbf{U}(Q)$, calculated with the use of three basis functions, Eq. (4), is found as (the basis functions are enumerated in the same order as in Eq. (4)):

$$\mathbf{U}(Q_A,Q_X,Q_Y) = \frac{M_E\omega_E^2}{2}(Q_x^2+Q_y^2)\mathbf{I} + \frac{M_A\omega_A^2}{2}Q_A^2\mathbf{I}$$

$$+\begin{pmatrix} \begin{array}{c}(-3J-g\beta H)/2+\delta\\ -\sqrt{6}(\lambda_E Q_X+\lambda_A Q_A)/4\end{array} & \sqrt{6}\lambda Q_Y/4 & -3D_l/4\sqrt{2} \\ \sqrt{6}\lambda Q_Y/4 & \begin{array}{c}(-3J-g\beta H)/2-\delta\\ -\sqrt{6}(-\lambda_E Q_X+\lambda_A Q_A)/4\end{array} & -3D_t/4\sqrt{2} \\ -3D_l/4\sqrt{2} & -3D_t/4\sqrt{2} & \begin{array}{c}3(J-g\beta H)/2+\delta\\ +\sqrt{6}\lambda_A Q_A\end{array} \end{pmatrix}.$$

$$(12)$$

The first two terms in Eq. (12) represent the elastic energy of the vibrations, ω_E and ω_A are the frequencies, M_E and M_A are the effective masses of the vibrations that are to be understood as the effective values for the vanadium triangle in the V_{15} structure, $\mathbf{I}$ is the 3×3 unit matrix. In general, the pseudo JT problem and corresponding symmetry lowering have a dynamic character. Later on for the sake of simplicity we will employ the adiabatic approximation so that the kinetic vibrational energy is omitted and therefore the eigen-values of the matrix, Eq. (12), can be associated with the full energies of the system.

For the sake of clarity the dynamical distortions (corresponding to a motion on the lower potential surface) will be considered separately from the static ones (J-strain), i.e. the analysis of the adiabatic surfaces will be done providing $\delta = 0$. First, the interaction with full-symmetric mode can not be eliminated by a simple shift of the normal coordinate Q_A to give a new equilibrium position that would be common for all spin states. This comes from the fact that the energy of the levels depend upon the parameter J that affects also the metal–metal distances through spin–vibronic interaction (mathematically this is a consequence of the fact that $\hat{V}_A$ is not represented by the unit matrix). Considering the adiabatic energies in the Q_A space one can see that the equilibrium positions of Q_A are different in the $S = 3/2$ and $S = 1/2$ spin states, $Q_A^0(S=3/2) = -Q_A^0(S=1/2) = \sqrt{6}\lambda/4M_A\omega_A$ which correspond to an effective increase of the size of the triangle while passing the crossover region toward high field. When the field passes through the crossover region the full-symmetric vibration changes its equilibrium configuration that means increase or decrease of the size of the symmetric triangle. This change occurs along with the JT deformations that lower the symmetry of the system. These structural transformations are mutually dependent and appear as a result of a complicated pseudo JT interaction involving three field dependent states coupled by three vibrational modes (in fact, the matrix $\hat{V}_A$ does not commute with both non-commuting matrices $\hat{V}_x$ and $\hat{V}_y$). Due to field dependence of the spin levels this interaction can be referred to as a magnetoelastic one. To simplify the problem we focus only on the JT structural transformations that are related to the most interesting effect of symmetry lowering and for this reason the full symmetric mode will be excluded (in this approximation we consider the section of the potential surfaces $U(Q_A,Q_x,Q_y)$ at $Q_A = 0$ that is the mean value for the two involved spin levels).

It is convenient to use the following dimensionless parameters: vibronic coupling $v = (\lambda/\hbar\omega)(\hbar/M\omega)^{1/2}$, vibrational coordinates $q_\alpha = (M_\alpha\omega/\hbar)^{1/2}Q_\alpha$ (in these variables the potential energy of the vibrations becomes $\sum_\alpha(\hbar\omega_\alpha/2)q_\alpha^2$), applied field $\xi = g\beta H/\hbar\omega$, and exchange parameters $j = J/\hbar\omega$, $\gamma_\alpha = (3/4)\sqrt{2}(D_\alpha/\hbar\omega)$, $\alpha = n$, l, t and $\omega \equiv \omega_E$. The whole Zeeman pattern of a triangular $S_i = 1/2$ cluster (provided that $\delta = 0$ and $\mathbf{H}\perp C_3$) is shown in Fig. 5a with the emphasis on the crossover region (Fig. 5b). Possible JT conformations are
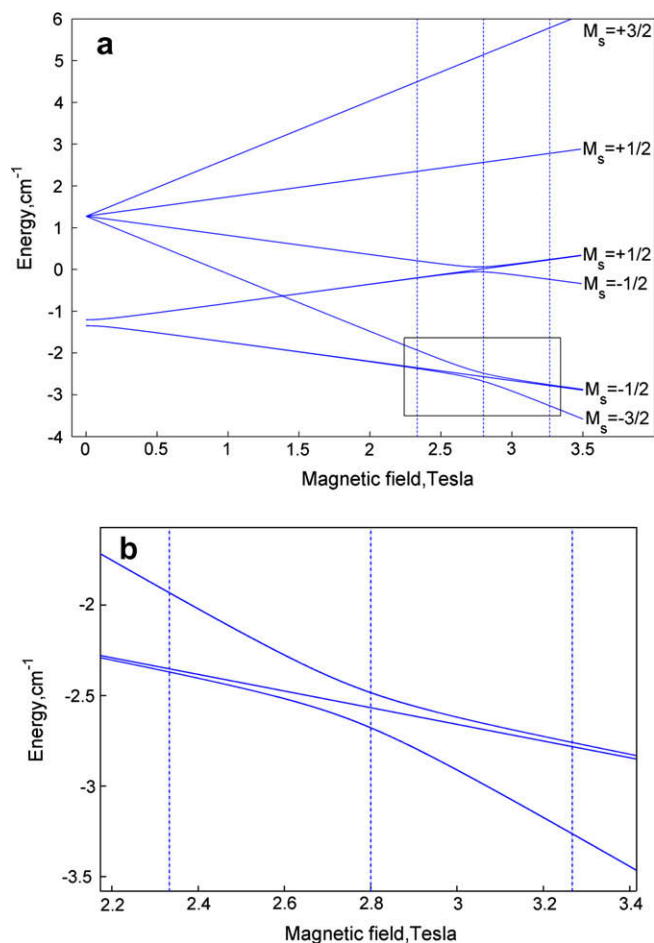
Fig. 5. Energy levels of a triangular $S_i = 1/2$ system in the perpendicular field ($\mathbf{H}\perp C_3$), static deformation is excluded, $J = 0.85$ cm^{-1}, $\delta = 0$, $D_n = 0.1J$, $D_t = 0.08J$, $D_l = 0.13J$, M_S labels correspond to a strong field limit. Three dashed vertical lines correspond (from left to right) to fields for which the adiabatic potentials are shown in Fig. 6a–d, respectively. (a) General pattern; (b) inset: three lowest levels in the vicinity of the anticrossing point.

determined by the interplay between two field dependent gaps and vibronic coupling. Fig. 6 illustrates some examples of the adiabatic surfaces of the system for a model set of parameters as functions of both the applied field and the vibronic coupling strength v. In the crossing point ($\xi = 3j$), the spectrum of spin levels consists of three equidistant levels (Fig. 5b, section marked by the central dashed line). Consequently, the symmetric (trigonal) system is stable providing weak vibronic coupling (Fig. 6a) that shows that the lowest sheet of the adiabatic surface has the only minimum in the point of highest symmetry or/and relatively strong AS exchange, meanwhile in the case of a relatively strong vibronic coupling and/or weak AS exchange the symmetric configuration of magnetic sites becomes unstable and the minima of the adiabatic surface are disposed at the ring of the trough (Fig. 6b). As distinguished from the static scalene distortion the JT conformations are dynamical in the sense that the motion along the ring of the trough corresponds to a series of isosceles configurations in which the spin frustration is eliminated.

Fig. 6c and d show the adiabatic potentials for the fields at the left ($\xi = \xi_l$) and at the right ($\xi = \xi_r$) of the crossing point correspondingly (left and right dashed lines) providing that the JT coupling is fixed. One can see that at $\xi \leqslant \xi_l$ the two low lying levels are nearly degenerate so that the condition for the JT instability persists irrespectively of coupling strength (Fig. 6c). On the contrary, on the
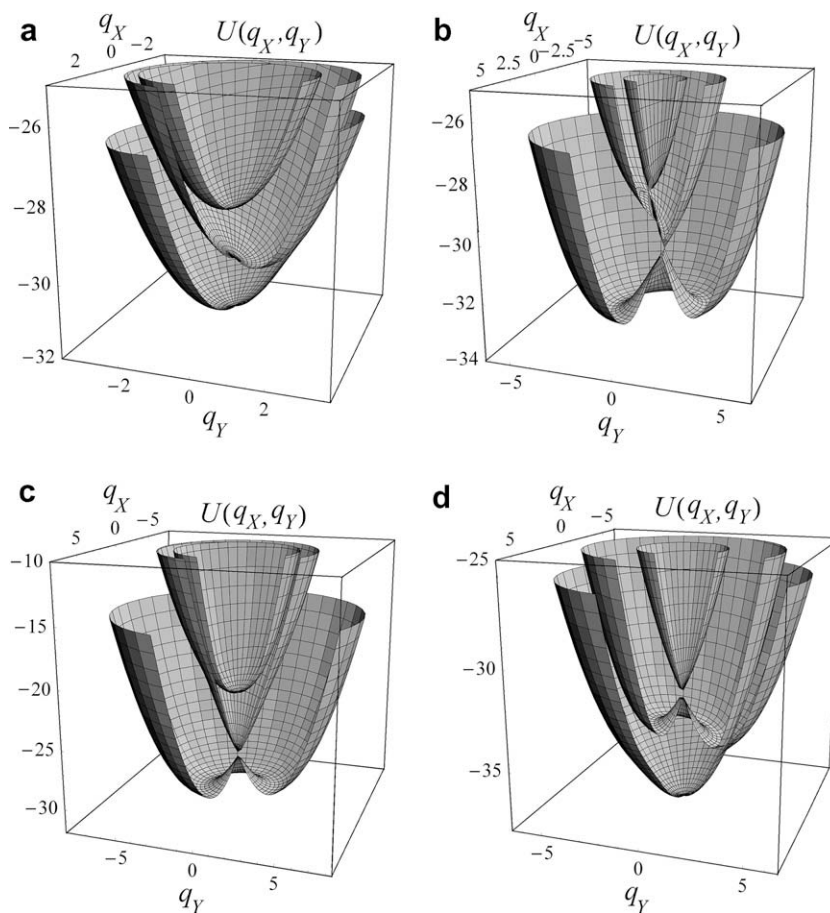
Fig. 6. Adiabatic surfaces of a triangular system, $j = 10$, $\gamma_l = \gamma_t = 0.1j$: (a) weak spin–vibronic coupling in the crossing point $\xi = 3j$, $\upsilon = j$, $\xi = 3j$; (b) strong spin–vibronic coupling in the crossing point $\xi = 3j$, $\upsilon = 4j$, $\xi = 3j$; (c) left of the crossing area, $\upsilon = 4j$, $\xi = 2.5j$; (d) strong magnetic field (right of the crossing area) $\upsilon = 4j$, $\xi = 3.5j$.

right of the crossing point ($\xi \geqslant \xi_r$) the lowest level is non-degenerate so in this case we are dealing with the pseudo JT effect. The instability can occur providing relatively strong coupling, otherwise the system remains stable as shown in Fig. 6c. Increase of the field tends to isolate non-degenerate level constraining thus instability. These results show that the structural conformations can be effectively controlled by the external magnetic field near the crossover region.

Estimation of the vibronic coupling parameters for V_{15} shows that for this system they are small as compared with the AS exchange and static distortions. The manifestations of the JT instability are expected to be significant for the triangular copper(II) clusters.

4. Magnetic susceptibility

In our recent paper [38], we have studied the shape of magnetization vs field in V_{15}. Since an additional parameter of distortion would bring an excessive flexibility the consideration in [38] was based on the model of a symmetric triangle. Keeping in mind the application to a wider set of the experimental data on V_{15} and different kinds of triangular systems we give here some sample calculations of susceptibility in order to demonstrate the main features of the distorted systems. Influence of the static distortions on the shape of the static susceptibility vs field in the anticrossing region is illustrated in Fig. 7. Within the isotropic model the low-temperature susceptibility has a narrow-pulse shape (Fig. 7a) corresponding to the exact crossing of $S = 3/2$, $M_S = -3/2$ and $S = 1/2$, $M_S = -1/2$ levels that gives rise to a sharp step of magnetization. Fig. 7a–c
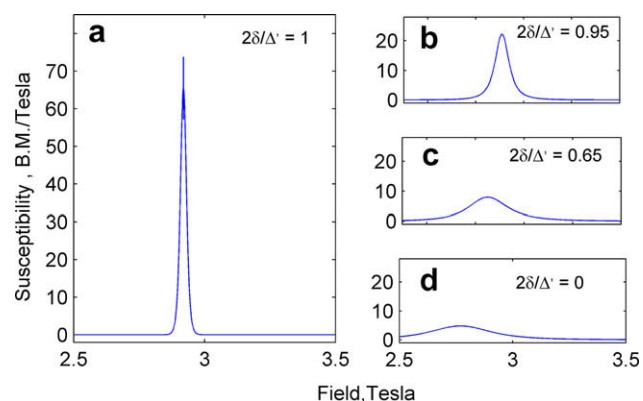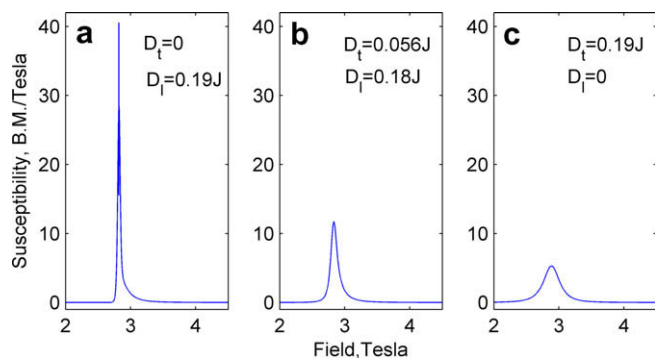

Fig. 7. Magnetic susceptibility in the perpendicular field at $T = 0.01$ K for the different ratios between $\delta \geqslant 0$ and AS provided fixed $\Delta' = 0.14$ cm^{-1}. $J = 0.85$ cm^{-1} and constant ratio $D_n{:}D_t{:}D_l = 1{:}2.12{:}2.12$ between the AS exchange components.

shows the effect of AS exchange providing a fixed zero-field gap Δ' while the ratio $2\delta/\Delta'$ is varied. With the increase of the contribution of the AS exchange the peak χ vs field becomes smoother thus showing that the static distortion reduces the AS exchange and consequently the magnetic anisotropy. On the other hand strong AS exchange reduces the effect of static distortion so these two interactions are competitive.

Fig. 8 shows variation of the susceptibility for $\delta > 0$ and different ratios of D_t and D_l providing that the value $\sqrt{D_l^2 + D_t^2}$ remains fixed. It is remarkable that in the presence of the scalene distortion the

Fig. 8. Magnetic susceptibility in the perpendicular field at $T = 0.01$ K, $J = 0.85$ cm^{-1}, $\delta = +0.054$ cm^{-1}, $D_n = 0.054$ cm^{-1}, $D_\perp = 0.162$ cm^{-1}, Δ' is fixed to 0.14 cm^{-1}.

two components of AS exchange affect χ vs field in essentially different ways. As one can see from Fig. 4a the exact crossing of the levels occurs in the ground state providing $D_t = 0$ (and $\delta > 0$) that gives rise to a sharp peak in $\chi(H)$ at low-temperature. The peak becomes smoother when the increase of D_t opens the gap (Fig. 4b) and finally, when $D_l = 0$ and D_t is maximal we arrive at a broad peak in $\chi(H)$ centered at $H_{cr} = 3J/g\beta$. Due to the mentioned symmetry rule for the energy pattern the dependence $\chi(H)$ for $\delta < 0$ varies in the opposite way, namely, the sharp peak is expected for $D_l = 0$, $D_t \neq 0$ and a broad peak at $D_l \neq 0$, $D_t = 0$ (see Fig. 4d–f). We could see that the ratio between the two in-plane AS components has a strong influence on the ground state behavior in the vicinity of the gap so this ratio influences the low-temperature susceptibility as well. Fig. 8 shows the susceptibility for different ratios between D_t and D_l providing a constant value of $D_\perp = \sqrt{D_t^2 + D_l^2}$ for positive δ.

These observations reveal also the role of the spin–vibronic JT coupling. In the case of strong coupling that results in the instability of the symmetric configuration the magnetic anisotropy caused by the AS exchange is expected to be reduced so in this limit one can expect a sharp step of magnetization. A similar result has been obtained for the low-field magnetization [39]). On the contrary when the AS exchange is strong enough the symmetric system remains stable and shows the magnetic anisotropy related to AS exchange. Thus the vibronic pseudo JT coupling that is magnetically isotropic affects the magnetic anisotropy through the reduction of the AS exchange.

5. Summary

In conclusion, we have reported the study of the Zeeman energy pattern of the trinuclear spin-frustrated system in the crossover region and have revealed a crucial role of the interplay between different components of AS exchange, static and dynamical JT distortions of the system. The pattern of adiabatic surfaces is qualitatively studied and the conditions for the field induced JT instability are discussed. It is shown that due to the magnetoelastic coupling the variation of the magnetic field near the crossover region can efficiently control the structural conformations. AS exchange from one side and structural and dynamical distortions from the other side are shown to be competitive. In our previous article [38], we have estimated two components of the AS exchange on the basis of the experimental data [19,43] on the static magnetization. In order to avoid overparametrization of the model (that would lead to an unstable fit) the deviation from the trigonal symmetry caused by the water molecule has been neglected. A complete set of the key magnetic parameters for V_{15} can be found through the analysis of a wider set of the experimental data, especially EPR. The discussion

of the experimental data on the INS and EPR spectra as well as on magnetization of V_{15} and in a series of spin-frustrated trinuclear systems based on the proposed model will be given elsewhere.

References

[1] D. Gatteschi, R. Sessoli, J. Villain, Molecular Nanomagnets, Oxford University Press, Oxford, 2006.
[2] R. Sessoli, D. Gatteschi, A. Caneschi, M.A. Novak, Nature 365 (1993) 141.
[3] D.D. Awschalom, D.P. Di Vencenzo, Phys. Today (1995) 43.
[4] B. Barbara, L. Gunter, Phys. World 12 (1999) 35.
[5] A. Caneschi, D. Gatteschi, R. Sessoli, A.-L. Barra, L.C. Brunel, M. Guillot, J. Am. Chem. Soc. 113 (1991) 5873.
[6] D. Gatteschi, A. Caneschi, L. Pardi, R. Sessoli, Science 265 (1994) 1054.
[7] D. Gatteschi, R. Sessoli, Angew. Chem. Int. Ed. 42 (2003) 268.
[8] N.E. Chakov, M. Soler, W. Wernsdorfer, K.A. Abboud, G. Christou, Inorg. Chem. 44 (2005) 5304.
[9] J.J. Borras-Almenar, J.M. Clemente-Juan, E. Coronado, A.V. Palii, B.S. Tsukerblat, Chem. Phys. 274 (2001) 145.
[10] J.J. Borras-Almenar, J.M. Clemente-Juan, E. Coronado, A.V. Palii, B.S. Tsukerblat, J. Solid State Chem. 159 (2001) 268.
[11] A.V. Palii, B.S. Tsukerblat, E. Coronado, J.M. Clemente-Juan, J.J. Borrás-Almenar, J. Chem. Phys 118 (2003) 5566.
[12] V.S. Mironov, L.F. Chibotaru, A. Ceulemans, J. Am. Chem. Soc. 125 (2003) 9750.
[13] A.V. Palii, S.M. Ostrovsky, S.I. Klokishner, B.S. Tsukerblat, J.R. Galán-Mascarós, C.P. Berlinguette, K.R. Dunbar, J. Am. Chem. Soc. 126 (2004) 16860.
[14] B.S. Tsukerblat, A.V. Palii, S.M. Ostrovsky, S.V. Kunitsky, S.I. Klokishner, K.R. Dunbar, J. Chem. Theory Comput. 1 (2005) 668.
[15] O. Waldmann, Chem. Phys. Lett. 332 (2000) 73.
[16] A.J. Legget, S. Chakravarty, A.T. Dorsey, P.A. Fisher, A. Garg, W. Zverger, Rev. Mod. Phys. 59 (1987) 1.
[17] V.V. Dobrovitski, M.I. Katsnelson, B.N. Harmon, Phys. Rev. Lett. 84 (2000) 3458.
[18] A. Müller, J. Döring, Angew. Chem. Int. Ed. Engl. 27 (1988) 1721.
[19] B. Barbara, J. Mol. Struct. 656 (2003) 135.
[20] I. Chiorescu, W. Wernsdorfer, A. Müller, H. Bögge, B. Barbara, Phys. Rev. Lett. 84 (2000) 3454.
[21] I. Chiorescu, W. Wernsdorfer, A. Müller, S. Miyashita, B. Barbara, Phys. Rev. B 67 (2003) 020402(R).
[22] S. Miyashita, J. Phys. Soc. Jpn. 65 (1996) 2734.
[23] H. Nojiria, T. Taniguchia, Y. Ajiro, A. Müller, B. Barbara, Physica B 346–347 (2004) 216.
[24] S. Miyashita, J. Phys. Soc. Jpn. 64 (1995) 3207.
[25] P.C.E. Stamp, I.S. Tupitsyn, Phys. Rev. B 69 (2004) 014401.
[26] A. Morello, P.C.E. Stamp, I.S. Tupitsyn, Phys. Rev. Lett. 97 (2006) 207206.
[27] G. Chaboussant, R. Basler, A. Sieber, S.T. Ochsenbein, A. Desmedt, R.E. Lechner, M.T.F. Telling, P. Kögerler, A. Müller, H.-U. Güdel, Europhys. Lett. 59 (2) (2002) 291.
[28] G. Chaboussant, S.T. Ochsenbein, A. Sieber, H.-U. Güdel, H. Mutka, A. Müller, B. Barbara, Europhys. Lett. 66 (3) (2004) 423.
[29] D. Gatteschi, L. Pardi, A.-L. Barra, A. Müller, J. Döring, Nature 354 (1991) 465.
[30] A.-L. Barra, D. Gatteschi, L. Pardi, A. Müller, J. Döring, J. Am. Chem. Soc. 114 (1992) 8509.
[31] D. Gatteschi, L. Pardi, A.-L. Barra, A. Müller, Mol. Eng. 3 (1993) 157.
[32] B.S. Tsukerblat, M.I. Belinskii, V.E. Fainzilberg, Magnetochemistry and spectroscopy of transition metal exchange clusters, in: M. Vol'pin (Ed.), Soviet Scientific Reviews B, Harwood Academic Publishers, 1987, pp. 337–482.
[33] I.E. Dzyaloshinsky, Zh. Exp. Teor. Fiz. 32 (1957) 1547.
[34] T. Moriya, Phys. Rev. 120 (1960) 91.
[35] B. Tsukerblat, A. Tarantul, A. Müller, Phys. Lett. A 353 (2006) 48.
[36] B. Tsukerblat, A. Tarantul, A. Müller, J. Chem. Phys. 125 (2006) 0547141.
[37] A. Tarantul, B. Tsukerblat, A. Müller, Chem. Phys. Lett. 428 (2006) 361.
[38] A. Tarantul, B. Tsukerblat, A. Müller, Inorg. Chem. 46 (2007) 161.
[39] B. Tsukerblat, A. Tarantul, A. Müller, J. Mol. Struct. 838 (2007) 124.
[40] M.I. Belinsky, The optimization of the composition, structure and properties of metals, oxides, composites, nano and amorphous materials, in: Proceedings of Sixth Israeli-Israeli Bi-National Workshop 2007, Israeli Academy of Sciences and Humanities, Jerusalem, 2007, p. 95.
[41] K.-Y. Choi, Y.H. Matsuda, H. Nojiri, U. Kortz, F. Hussain, A.C. Stowe, C. Ramsey, N.S. Dalal, Phys. Rev. Lett. 96 (2006) 107202.
[42] T. Yamase, E. Ishikawa, K. Fukaya, H. Nojiri, T. Taniguchi, T. Atake, Inorg. Chem. 43 (2004) 8150.
[43] I. Chiorescu, W. Wernsdorfer, A. Müller, H. Bögge, B. Barbara, Magn. Magn. Mater. 221 (2000) 103.
[44] J. Yoon, L.M. Mirica, T.D.P. Stack, E.I. Solomon, J. Am. Chem. Soc. 126 (2004) 12586.
[45] Y. Sanakis, A.L. Macedo, I. Moura, Jose J.G. Moura, V. Papaefthymiou, E. Münck, J. Am. Chem. Soc. 122 (2000) 11855–11863.

[46] A.K. Boudalis, Y. Sanakis, F. Dahan, M. Hendrich, J.-P. Tuchagues, Inorg. Chem. 45 (2006) 443.

[47] B. Cage, F.A. Cotton, N.S. Dalal, E.A. Hillard, B. Rakvin, C.M. Ramsey, J. Am. Chem. Soc. 125 (2003) 5270.

[48] O. Waldmann, C. Dobe, S.T. Ochsenbein, H.-U. Güdel, I. Sheikin, Phys. Rev. Lett. 96 (2006) 027206.

[49] R. Englman, The Jahn–Teller Effect in Molecules and Crystals, Wiley, London, 1972.

[50] I.B. Bersuker, V.Z. Polinger, Vibronic Interactions in Molecules and Crystals, Springer-Verlag, Berlin, 1989.

[51] I.B. Bersuker, The Jahn–Teller Effect, Cambridge University Press, 2006.

[52] B.S. Tsukerblat, Group Theory in Chemistry and Spectroscopy, Dover, Mineola, NY, 2006.